

Supporting Information

Stable and metallic two-dimensional TaC₂ as an anode material for lithium-ion battery

Tong Yu, Shoutao Zhang, Fei Li, Ziyuan Zhao, Lulu Liu, Haiyang Xu,* and Guochun Yang*

Centre for Advanced Optoelectronic Functional Materials Research and Key Laboratory for UV Light-Emitting Materials and Technology of Ministry of Education, Northeast Normal University, Changchun 130024, China

*Address correspondence to: hyxu@nenu.edu.cn; yanggc468@nenu.edu.cn

Index	page
1. Computational details	2
2. Structural comparison between two-dimensional (2D) and bulk TaC	4
3. The structures of TaC ₃ and TaC ₄ monolayers	4
4. Band structures of TaC ₂ , TaC and Ta ₂ C monolayers	5
6. All the possible configurations of TaC ₂ Li ₂	6
7. Thermal stability and electron localization function (ELF) of TaC ₂ Li ₄	7
8. The most stable adsorption configurations of Ta ₂ C	8
9. Structural information of the predicted Ta _x C _y monolayers	9
10. References	10

Computational Details

The particle swarm optimization (PSO) method within the evolutionary algorithm as implemented in the Crystal structure AnaLYsis by Particle Swarm Optimization (CALYPSO) code was employed to find the low energy structures of Ta_xC_y ($x = 1$ and $y = 1 - 4$, or $x = 2$ and $y = 1$) monolayers.^[1,2] Unit cells containing 1, 2 and 4 formula units (f.u.) were considered. In the first step, random structures with certain symmetry are constructed in which atomic coordinates are generated by the crystallographic symmetry operations. Local optimizations using the VASP code^[3] were done with the conjugate gradients method and stopped when Gibbs free energy changes became smaller than 1×10^{-5} eV per cell. After processing the first generation structures, 60% of them with lower Gibbs free energies are selected to construct the next generation structures by PSO. 40% of the structures in the new generation are randomly generated. A structure fingerprinting technique of bond characterization matrix is applied to the generated structures, so that identical structures are strictly forbidden. These procedures significantly enhance the diversity of the structures, which is crucial for structural global search efficiency. In most cases, structural searching simulations for each calculation were stopped after generating 1000 ~ 1200 structures (e.g., about 20 ~ 30 generations).

The local structural relaxations and electronic properties calculations were performed in the framework of the density functional theory (DFT)^[4] within the generalized gradient approximation (GGA)^[5] parametrized as implemented in the VASP code. The cut-off energy for the expansion of wavefunctions into plane waves was set to 700 eV in all calculations except the lithiation process (400 eV). According to the Monkhorst-Pack scheme,^[6] a $16 \times 16 \times 1$ Γ -centered k-point meshes were selected for the structural optimization and electronic properties calculations, and a $5 \times 5 \times 2$ k-point grids were used during the lithiation process.

Phonon dispersion calculations were performed for $3 \times 5 \times 1$, $2 \times 2 \times 1$, and $4 \times 4 \times 1$ supercell for TaC_2 , TaC , and Ta_2C , respectively, which was based on a supercell approach as done in the Phonopy code.^[7] First-principles molecular dynamics (MD)^[8]

simulations for large $4 \times 4 \times 1$ (TaC_2), $3 \times 3 \times 1$ (TaC), and $5 \times 5 \times 1$ (Ta_2C) supercell were performed at different temperatures of 300 K, 500 K, and 1000 K. MD simulation in NVT ensemble lasted for 10 ps with a time step of 1.0 fs. The temperature was controlled by using the Nosé-Hoover method.

Supporting Figures

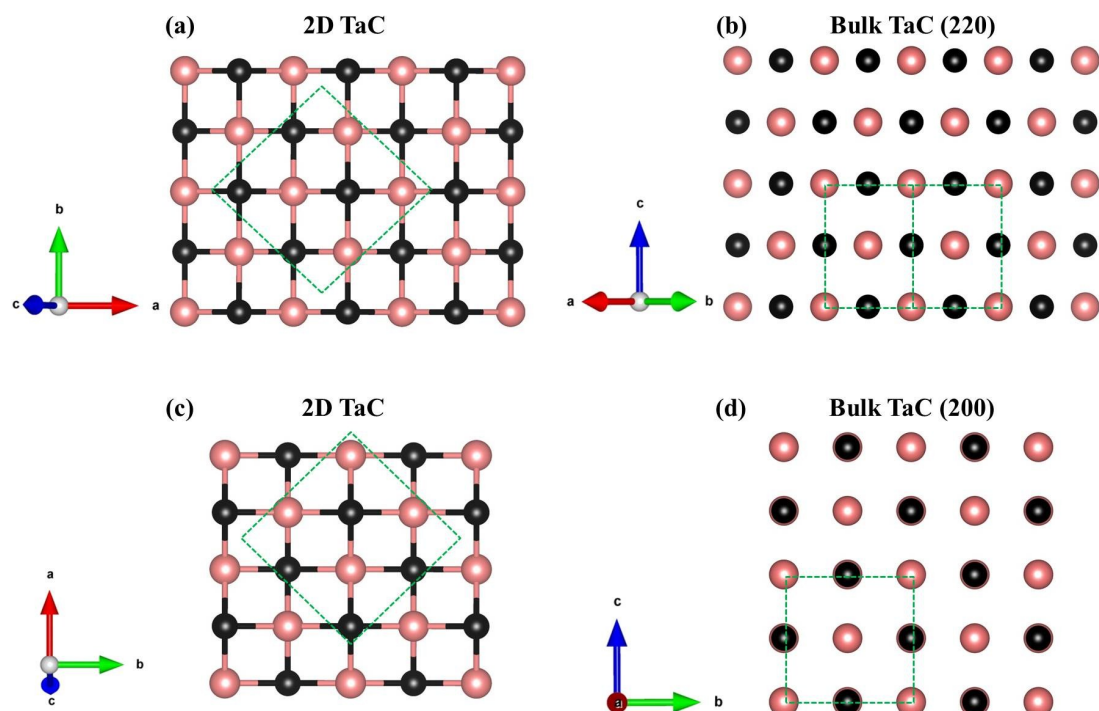


Figure S1. Comparison between (a, c) 2D TaC monolayer and lattice planes (b) (220), (d) (200) of bulk TaC. Dashed lines represent unit cell.

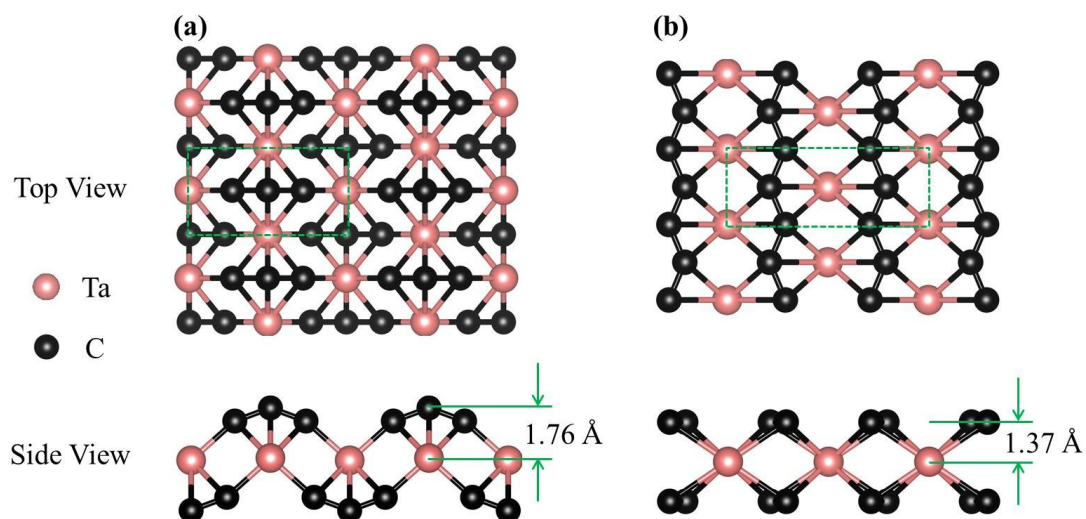


Figure S2. The top and side views of the lowest-energy structures of (a) TaC₃ and (b) TaC₄. Dashed lines represent unit cell.

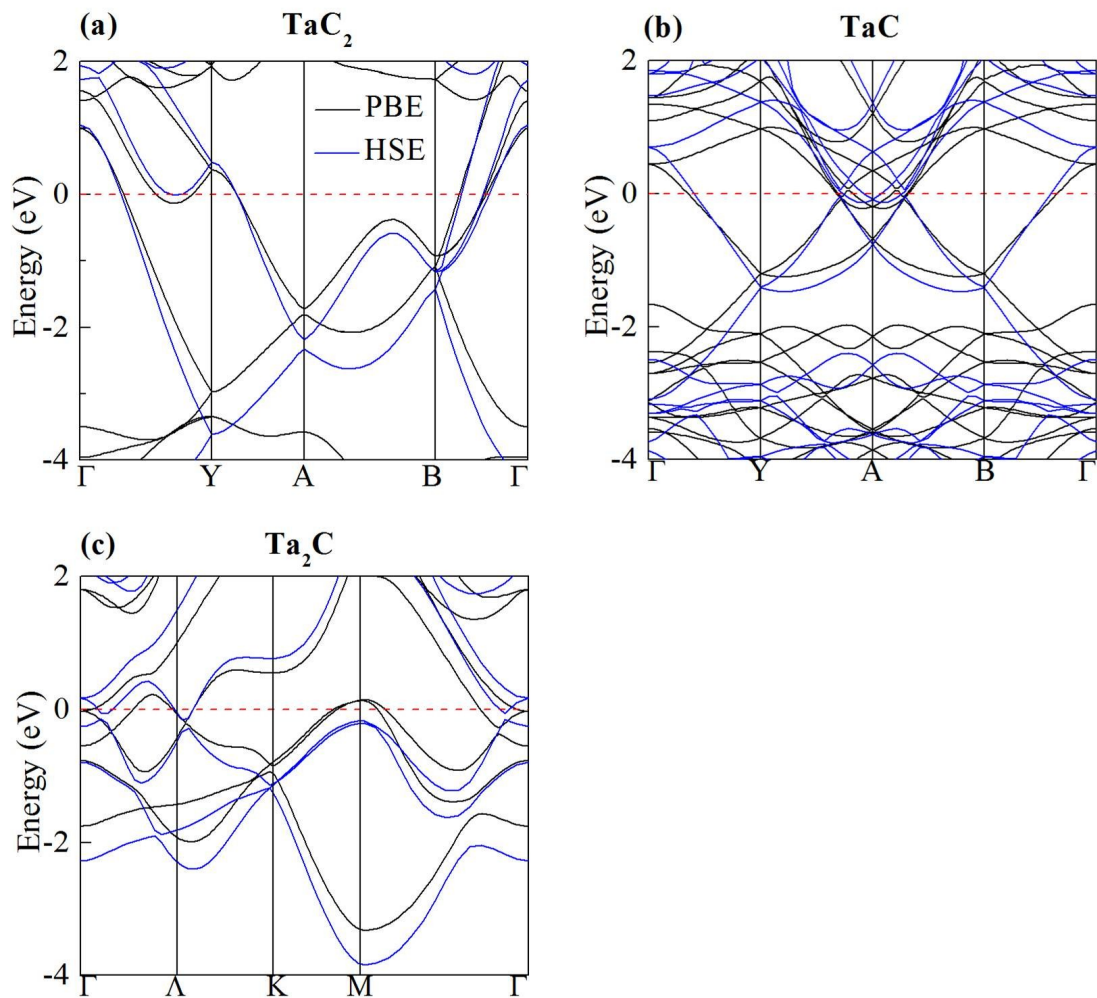


Figure S3. Band structures of TaC_2 (a), TaC (b), and Ta_2C (c) monolayers calculated at PBE and HSE levels of theory, respectively. Red dashed lines represent Fermi level.

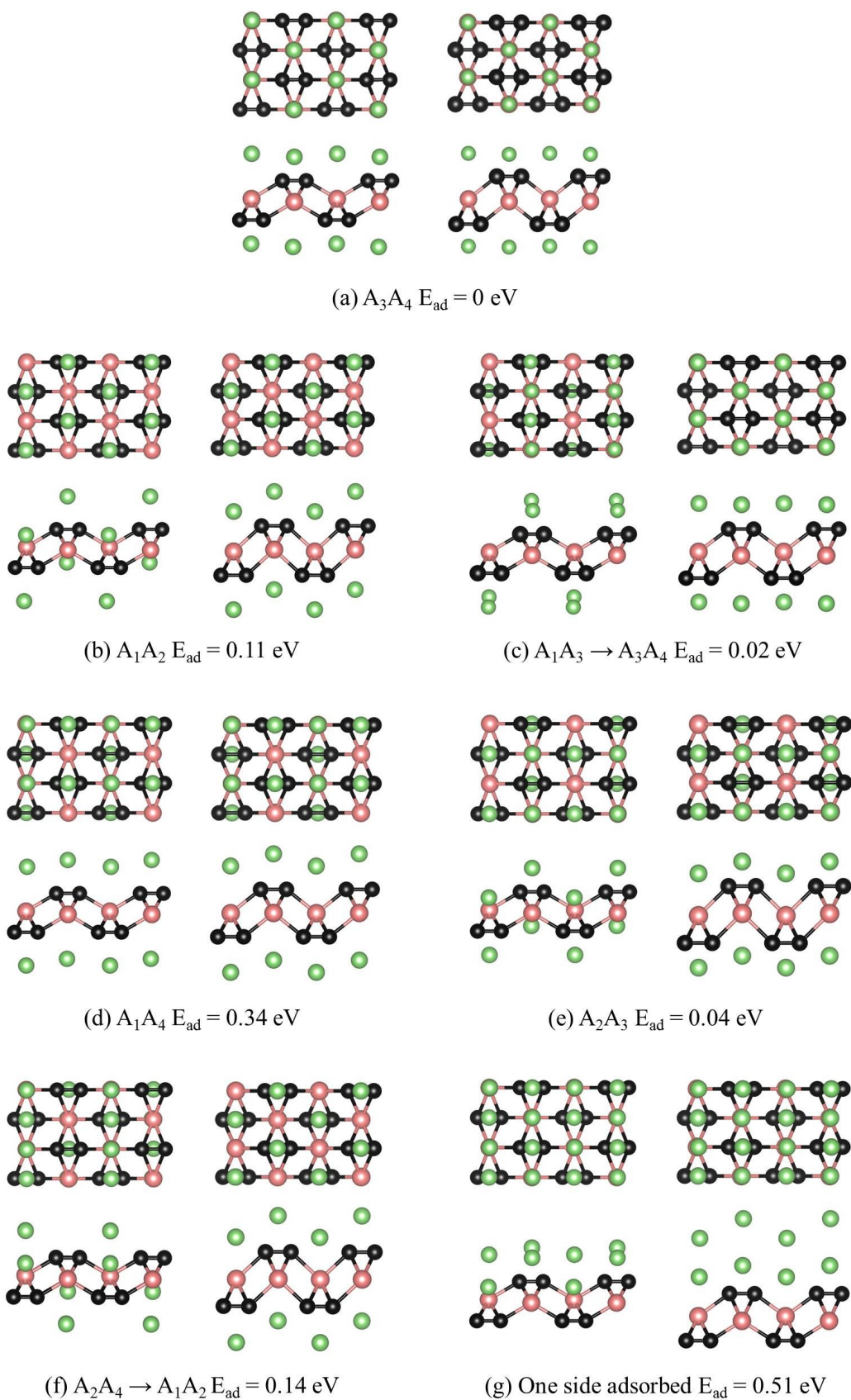


Figure S4. The calculated initial (left) and optimized (right) structures of TaC_2Li_2 and their relative energies with respect to the lowest energy configuration A_3A_4

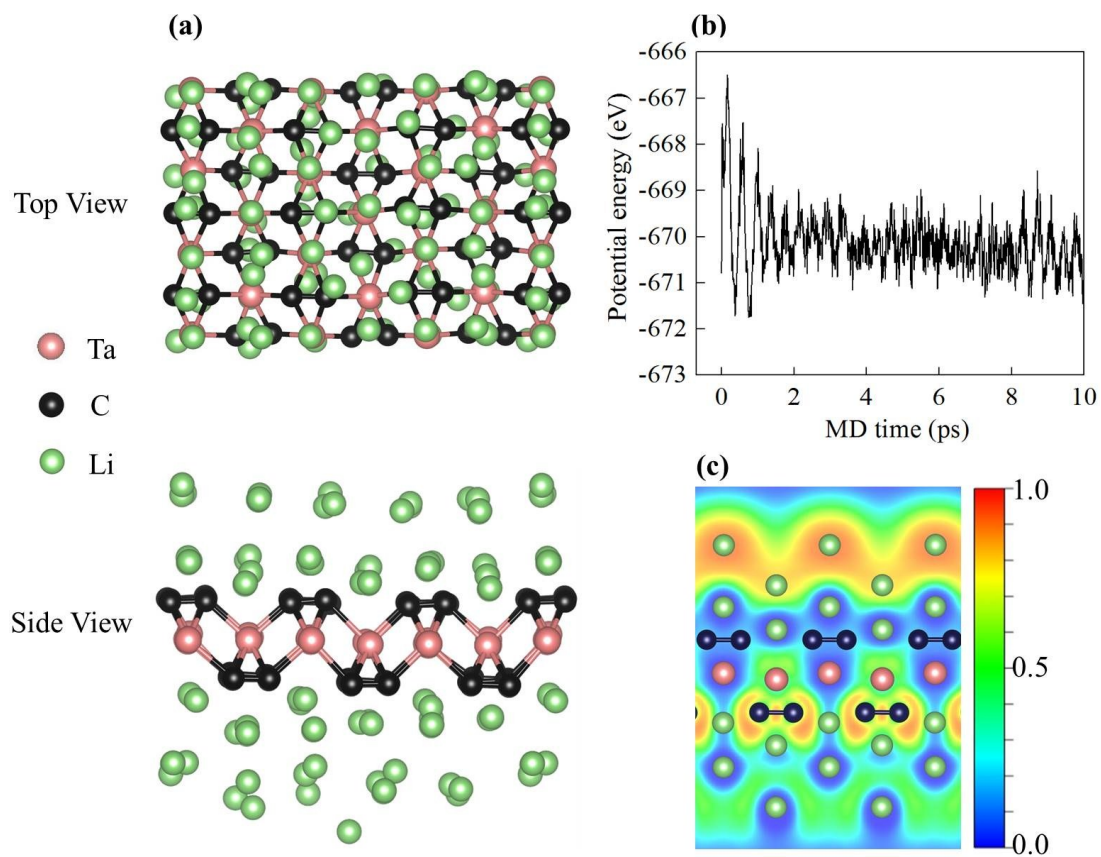


Figure S5. (a) Snapshots after equilibration, (b) total potential energy as a function of MD time at temperature of 300 K and (c) ELF slice of TaC₂Li₄.

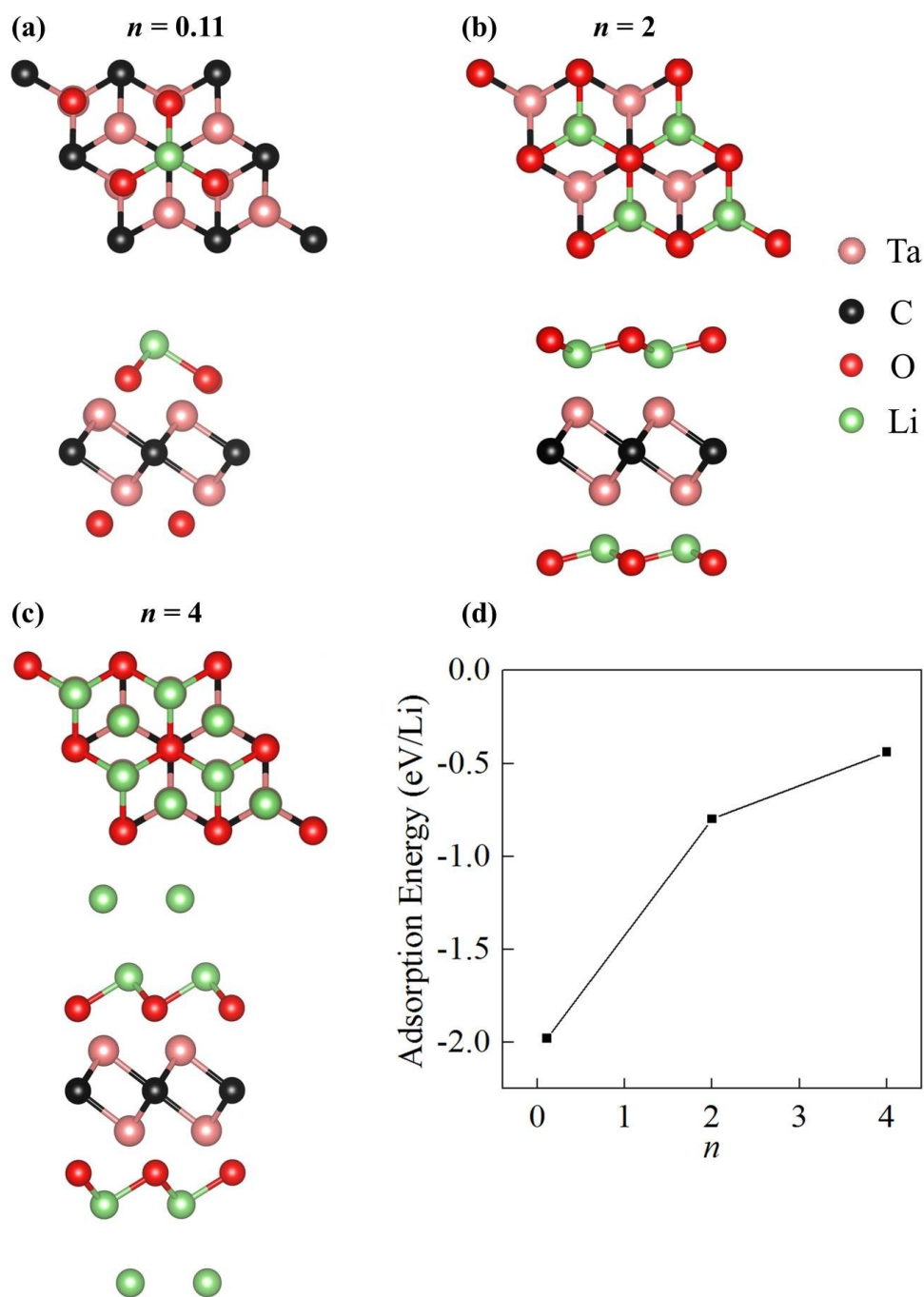


Figure S6. (a)-(c) The most stable structures with different Li concentrations in $\text{Ta}_2\text{CO}_2\text{Li}_n$. The n values are 0.11, 2, and 4. (d) The adsorption energies as a function of Li concentration.

Supporting Tables

Table S1. Structural information of the predicted Ta_xC_y ($x = 1$ and $y = 1 - 4$, or $x = 2$ and $y = 1$) monolayers.

Phase	Space Group	Lattice		Wyckoff Positions		
		Parameters	Atoms	(fractional)		
		(Å, °)		x	y	z
TaC ₂	$P2_1/m$	$a = 4.95402$	Ta(2e)	-0.24986	0.25000	0.49590
		$b = 3.47991$	C(2e)	0.39055	0.25000	0.44894
		$c = 22.41107$	C(2e)	-0.11273	0.75000	0.55106
		$\alpha = \gamma = 90.00000$				
		$\beta = 89.60196$				
TaC	Cm	$a = 7.65550$	Ta(4b)	0.53115	-0.24998	0.49077
		$b = 8.47400$	Ta(2a)	0.30214	-0.50000	0.50917
		$c = 21.77430$	Ta(2a)	0.80229	-0.50000	0.50931
		$\alpha = \gamma = 90.00000$	C(2a)	0.00270	-0.50000	0.46595
		$\beta = 113.63800$	C(2a)	0.50296	-0.50000	0.46598
			C(4b)	0.33047	-0.25007	0.53402
Ta ₂ C	$P-3m1$	$a = b = 3.08120$	Ta(2d)	0.33333	0.66667	-0.54412
		$c = 27.50710$	C(1b)	0.00000	2.00000	-0.50000
		$\alpha = \gamma = 90.00000$				
		$\beta = 120.00000$				
TaC ₃	$Pmmn$	$a = 3.10300$	Ta(2b)	0.00000	0.50000	0.50226
		$b = 5.56740$	C(2a)	0.00000	0.00000	0.39966
		$c = 17.97860$	C(4e)	0.00000	0.22461	0.42543
		$\alpha = \beta = \gamma = 90.00000$				
TaC ₄	$Cmm2$	$a = 2.59980$	Ta(2a)	0.00000	0.00000	0.49797
		$b = 6.94930$	C(4e)	0.00000	0.71045	0.56717
		$c = 19.73570$	C(4e)	0.00000	0.71050	0.42884
		$\alpha = \beta = \gamma = 90.00000$				

References

- [1] Y. Wang, J. Lv, L. Zhu, Y. Ma, *Comput. Phys. Commun.* **2012**, *183*, 2063.
- [2] Y. Wang, J. Lv, L. Zhu, Y. Ma, *Phys. Rev. B.* **2010**, *82*, 94116.
- [3] G. Kresse, J. Furthmu, *Phys. Rev. B.* **1996**, *54*, 11169.
- [4] W. KOHN, L. J. SHAM, *Phys. Rev* **1965**, *140*, A1133.
- [5] J. P. Perdew, K. Burke, M. Ernzerhof, *Phys. Rev. Lett.* **1996**, *77*, 3865.
- [6] H. J. Monkhorst, J. D. Pack, *Phys. Rev. B.* **1976**, *13*, 5188.
- [7] A. Togo, F. Oba, I. Tanaka, *Phys. Rev. B.* **2008**, *78*, 134106.
- [8] G. J. Martyna, M. L. Klein, M. Tuckerman, *J. Chem. Phys.* **1992**, *97*, 2635.